



ANIMAL MODELS

Mammalian Target of Rapamycin Complex 1 and Cyclooxygenase 2 Pathways Cooperatively Exacerbate Endometrial Cancer

Takiko Daikoku,^{*} Jumpei Terakawa,^{*} Md M. Hossain,[†] Mikihiro Yoshie,^{*} Monica Cappelletti,[‡] Peiying Yang,[§] Lora H. Ellenson,[¶] and Sudhansu K. Dey^{*}

From the Division of Reproductive Sciences,^{*} Perinatal Institute, and the Divisions of Biostatistics and Epidemiology[†] and Molecular Immunology,[‡] Cincinnati Children's Hospital Medical Center, Cincinnati, Ohio; the Department of Cancer Biology,[§] University of Texas MD Anderson Medical Cancer Center, Houston, Texas; and the Department of Pathology and Laboratory Medicine,[¶] New York Presbyterian Hospital—Weill Cornell Medical College, New York, New York

Accepted for publication
May 28, 2014.

Address correspondence to
Takiko Daikoku, Ph.D., or
Sudhansu K. Dey, Ph.D.,
Cincinnati Children's Hospital
Medical Center, Division of
Reproductive Sciences, MLC
7045, 3333 Burnet Ave.,
Cincinnati, OH 45229-3039. E-
mail: takiko.daikoku@cchmc.org
or sk.dey@cchmc.org.

The underlying causes of endometrial cancer (EMC) are poorly understood, and treatment options for patients with advanced stages of the disease are limited. Mutations in the phosphatase and tensin homologue gene are frequently detected in EMC. Cyclooxygenase 2 (Cox2) and mammalian target of rapamycin complex 1 (mTORC1) are known downstream targets of the phosphatase and tensin homologue protein, and their activities are up-regulated in EMC. However, it is not clear whether Cox2 and mTORC1 are crucial players in cancer progression or whether they work in parallel or cooperatively. In this study, we used a Cox2 inhibitor, celecoxib, and an mTORC1 inhibitor, rapamycin, in mouse models of EMC and in human EMC cell lines to explore the interactive roles of Cox2 and mTORC1 signaling. We found that a combined treatment with celecoxib and rapamycin markedly reduces EMC progression. We also observed that rapamycin reduces Cox2 expression, whereas celecoxib reduces mTORC1 activity. These results suggest that Cox2 and mTORC1 signaling is cross-regulated and cooperatively exacerbate EMC. (*Am J Pathol* 2014, 184: 2390–2402; <http://dx.doi.org/10.1016/j.ajpath.2014.05.023>)

Endometrial cancer (EMC) is the most common gynecological malignancy among American women.^{1,2} According to National Cancer Institute estimates, about 50,000 women will be diagnosed with EMC in 2013 and approximately 8200 patients are likely to die from it. Underlying causes of EMC are not clearly understood, and treatment options for patients with advanced stages are limited.^{1,2} Several genetic alterations are associated with EMC.^{1,2} One of the most common mutations is in the phosphatase and tensin homologue gene (*PTEN*). Mutations of the *TP53* gene, which encodes p53, are also found in EMC and primarily occur in poorly differentiated carcinomas.^{1,2}

The loss of *PTEN* results in increased phosphoinositide 3-kinase (PI3K) activity and thymoma viral proto-oncogene 1 (Akt) activation. Increased levels of phosphorylated (activated) Akt (pAkt) stimulate cyclooxygenase 2 (Cox2) and mammalian target of rapamycin complex 1 (mTORC1) activities.^{3–9} Heightened Cox2 and mTORC1 signaling are

associated with EMC.^{9–14} Cox2 is overexpressed in many solid tumors, and Cox2-derived prostaglandins (PGs), especially PGE₂ via its receptors EP₂/EP₄, significantly contribute to carcinogenesis.^{15,16} Interestingly, analogues of rapamycin and related inhibitors of mTORC1 signaling are in phase I to II clinical trials to treat EMC, and the beneficial effects of celecoxib in cancers are also the subject of current clinical trials (<http://www.clinicaltrials.gov>, last accessed July 22, 2014).

Animal models of spontaneously developed cancers are powerful tools for studying the mechanisms underlying cancer initiation and progression and for developing treatment strategies. We previously generated mouse models with conditional uterine deletion of *Pten* (*Pten*^{Δd}) or of *Pten*

Supported in part by grants from the National Cancer Institute, NIH (P01-CA-77839) (S.K.D.) and Ohio Cancer Research Associates (T.D.) and postdoctoral fellowships from the Japan Society for the Promotion of Science (J.T.).

Disclosures: None declared.

and *Trp53* (*Pten/Trp53^{ΔΔ}*) using the Cre/loxP approach.¹⁷ Female mice with floxed alleles of *Pten* and/or *Trp53* were crossed with males expressing Cre recombinase driven under the progesterone receptor promoter (*Pgr-Cre*).¹⁸ *Pten^{ΔΔ}* females spontaneously developed EMC with 100% penetrance by 30 days of age, and *Pten/Trp53^{ΔΔ}* females developed a more aggressive form of this disease by 21 days of age. Using these mouse models, we previously showed that pAkt and Cox2 levels are elevated in the uteri of both *Pten^{ΔΔ}* and *Pten/Trp53^{ΔΔ}* mice.¹⁷

Here, we show that a downstream component of the mTORC1 effector pathway is significantly up-regulated in the uteri of these mice. These results suggest that Cox2 and mTORC1 are associated with EMC. We then examined whether the Cox2 and mTORC1 pathways are critical in cancer progression and whether they influence EMC independently or cooperatively. We treated *Pten^{ΔΔ}* females and their control littermates (*Pten^{fl/fl}*) with rapamycin (mTORC1 inhibitor) and/or celecoxib (Cox2 inhibitor) by oral gavage on every alternate day for 29 days, beginning at 30 days of age. We found that treatment with rapamycin or celecoxib monotherapy attenuated tumor growth, whereas maximal reductions in tumor growth and progression were noted in *Pten^{ΔΔ}* females receiving both rapamycin and celecoxib. We also observed a similar reduction in tumor progression in *Pten/Trp53^{ΔΔ}* females after combined treatment with rapamycin and celecoxib. Using a mouse EMC cell line established from *Pten/Trp53^{ΔΔ}* uteri and three human EMC cell lines, we also found that rapamycin reduces Cox2 expression at the mRNA and protein levels and that celecoxib reduces mTORC1 activity, suggesting that Cox2 and mTORC1 activities are cross-regulated and cooperatively exacerbate EMC. Thus, a combined treatment with celecoxib and rapamycin could be an effective therapeutic strategy for combating EMC.

Materials and Methods

Mice

Mice with uterine deletion of *Pten* (*Pten^{loxP/loxP}/Pgr^{cre/+}* = *Pten^{ΔΔ}*), both *Pten* and *Trp53* (*Pten^{loxP/loxP}/Trp53^{loxP/loxP}/Pgr^{cre/+}* = *Pten/Trp53^{ΔΔ}*), or tuberous sclerosis 1 (*Tsc1^{loxP/loxP}/Pgr^{cre/+}* = *Tsc1^{ΔΔ}*) were generated as described previously.^{17,19} For experiments, littermate *Pten^{ΔΔ}* and *Pten/Trp53^{ΔΔ}* females on the mixed background were used. An mTORC1 selective inhibitor (rapamycin) and/or a Cox2 selective inhibitor (celecoxib) were suspended in 10% polyethylene glycol 400 (PEG400) and 10% (v/v) polysorbate 80 in water by constant stirring. Mice were treated with vehicle (10% PEG400 and 10% polysorbate 80), 5 mg/kg body weight of rapamycin, 20 mg/kg body weight of celecoxib, or 5 mg/kg body weight of rapamycin plus 20 mg/kg body weight of celecoxib, by oral gavage every alternate day from 30 to 59 days of age.^{20–29} Stages of the estrous cycle were identified by the examination of vaginal smears. All mice used in this investigation were housed in barrier facilities in the Animal

Care Facility at Cincinnati Children's Hospital Medical Center according to NIH and institutional guidelines for the care and use of laboratory animals. All protocols were reviewed and approved by the Institutional Animal Care and Use Committee, Cincinnati Children's Research Foundation.

Treatment with Progesterone or Estrogen

To assess the effects of ovarian hormones on uterine phosphorylated ribosomal protein S6 (pS6) expression, CD1 wild-type (WT) females were ovariectomized and rested for 2 weeks. They were given a single injection of progesterone (P_4 , 2 mg/mouse, s.c.) or 25 or 100 ng estradiol-17 β (E_2).³⁰ The control group of mice received only the vehicle (oil). Mice were euthanized after 12 hours, and uteri were collected for immunohistochemistry (IHC) analysis.

Scoring Cancer Severity

The extent of the carcinoma was subjectively measured based on the amount of disease in the uterus, as measured by light microscopic examination of hematoxylin and eosin stains as well as IHC analysis for cytokeratin 8 (CK8) (score: 0, no carcinoma; 1, $\leq 25\%$; 2, 26% to 50%; 3, 51% to 75%; or 4, 76% to 100%) of the endometrium involved by carcinoma. Myometrial invasion was noted but was not included in the scoring system.

Establishment and Culture of Mouse EMC Cell Line

Mouse uterine epithelial cells were isolated by following the previously described methods.^{30–32} In brief, uteri collected from 2-month-old *Pten^{ΔΔ}* or *Pten/Trp53^{ΔΔ}* mice were cleaned of fat tissue, slit longitudinally, and cut into pieces 2 to 3 mm in length. Uterine pieces were then washed several times with phenol red–free Hank's Balanced Salt Solution (Life Technologies Corporation, Carlsbad, CA) with 100 μ g/mL of streptomycin, 100 U/mL of penicillin, and 2.5 μ g/mL of amphotericin B (Sigma-Aldrich, St. Louis, MO). Tissues were digested with 6 mg/mL of dispase (Life Technologies) and 25 mg/mL pancreatin (Sigma-Aldrich) for 1 hour at 4°C, 1 hour at room temperature, and 10 minutes at 37°C. After these digestion steps, tissues were immediately diluted in Hank's Balanced Salt Solution containing 10% fetal bovine serum (FBS) and mixed thoroughly to dislodge the sheet of luminal epithelial cells. The dispersed cells were collected by centrifugation and plated on the dish were coated with Matrigel, which was diluted to 4 \times with phosphate-buffered saline (PBS) (BD 354234; BD Biosciences, San Jose, CA). Cells were cultured in Dulbecco's modified Eagle's medium and Ham's F-12 nutrient mixture (1:1) with 10% FBS and antibiotics.

Immunolocalization

Immunofluorescence was performed to localize E-cadherin and CK8, along with nuclear staining as previously described.³³

Senescence-Associated β -Gal Staining

Staining of senescence-associated β -gal activity was performed as described previously.²¹ In brief, cultured cells were fixed in 0.5% glutaraldehyde in PBS and stained overnight in PBS (pH 5.5) containing 1 mmol/L $MgCl_2$, 1 mg/mL X-Gal, and 5 mmol/L each of potassium ferricyanide and potassium ferrocyanide. Cells were counterstained with eosin.

Culture of Human EMC Cell Lines

RL95-2 was purchased from ATCC (Manassas, VA). HEC116 and HEC50B were kindly provided by Hiroyuki Kuramoto (Kitasato University, Kanagawa, Japan). RL95-2 was cultured in Dulbecco's modified Eagle's medium and Ham's F-12 nutrient mixture (1:1), whereas HEC116 and HEC50B were cultured in Dulbecco's modified Eagle's medium. All culture media were supplemented with 10% FBS and antibiotics.

Western Blot Analysis

Tissue and cultured cell samples were prepared as previously described.³⁴ After measuring of protein concentrations, supernatants were boiled with SDS-PAGE sample buffer for 5 minutes. Samples were run on 10% to 12% SDS-PAGE gels and transferred onto polyvinylidene difluoride membranes. Membranes were blocked with 10% milk or 5% bovine serum albumin in Tris-buffered saline Tween20 and probed with antibodies to S6 and pS6 (Cell Signaling Technology, Inc., Beverly, MA), Cox1 (kindly provided by David DeWitt, Michigan State University, East Lansing, MI), Cox2 (Cayman Chemical Company, Ann Arbor, MI), Akt (Cell Signaling Technology, Inc.), pAkt (Cell Signaling Technology, Inc.),

E-cadherin (Cell Signaling Technology, Inc.), or β -actin (Santa Cruz Biotechnology, Inc., Dallas, TX), overnight at 4°C (Table 1). After washing, blots were incubated in peroxidase-conjugated donkey antgoat or donkey antirabbit IgG (Jackson ImmunoResearch Laboratories, Inc., West Grove, PA). All signals were detected using chemiluminescent reagents (GE Healthcare, Wauwatosa, WI). S6, Akt, and β -actin served as loading controls.

IHC Analysis

IHC analysis was performed as previously described.^{22,34} Tissues were fixed in Protocol Safefix II (Thermo Fisher Scientific Inc.) and embedded in paraffin. Uterine sections (6 μ) were subjected to immunostaining using antibodies to pS6 (Cell Signaling Technology, Inc.), mTOR (Cell Signaling Technology, Inc.), raptor (Cell Signaling Technology, Inc.), CK8 (Developmental Studies Hybridoma Bank, Iowa City, IO), Ki-67 (Thermo Fisher Scientific Inc.), or active caspase 3 (Cell Signaling Technology, Inc.) (Table 1). After deparaffinization and hydration, sections were subjected to antigen retrieval by autoclaving in 10 mmol/L sodium citrate solution (pH 6) for 10 minutes. A diaminobenzidine was used to visualize antigens. Sections were counterstained with hematoxylin and eosin.

PG Assays

Uterine tissue was collected and analyzed for PG levels using a modified method described previously.³⁵ In brief, approximately 20- to 25-mg frozen tissues were homogenized in 400 μ L of PBS (0.1% BHT and 1 mmol/L EDTA) using a Precellys high-throughput tissue homogenizer coupled with a Cryolys cooling unit (Bertin Corporation,

Table 1 Antibodies and Applications

Antibody	Source	Catalog number	Use	Dilution
pS6	Cell Signaling Technology, Inc.	2211	WB (12% gel)	1:2000
pS6	Cell Signaling Technology, Inc.	2211	IHC	1:200
S6	Cell Signaling Technology, Inc.	2217	WB (12% gel)	1:2000
mTOR	Cell Signaling Technology, Inc.	2983	IHC	1:100
Raptor	Cell Signaling Technology, Inc.	2280	IHC	1:50
CK8	Developmental Studies Hybridoma Bank	TROMA-1	IHC	1:25
CK8	Developmental Studies Hybridoma Bank	TROMA-1	IF/IC	1:200
Ki-67	Thermo Fisher Scientific, Inc.	RM-9106	IHC	1:200
Cleaved caspase 3	Cell Signaling Technology, Inc.	9661	IHC	1:300
Cleaved caspase 3	Cell Signaling Technology, Inc.	9661	IF/IC	1:400
pAkt	Cell Signaling Technology, Inc.	3787	WB (10% gel)	1:1000
Akt	Cell Signaling Technology, Inc.	9272	WB (10% gel)	1:1000
β -actin	Santa Cruz Biotechnology, Inc.	sc-1615	WB (10% gel)	1:500
Cox1	David DeWitt (East Lansing, MI)	NA	WB (10% gel)	1:2500
Cox2	Cayman Chemical Company	160126	WB (10% gel)	1:5000
E-cadherin	Cell Signaling Technology, Inc.	3195	IF/IC	1:400
Hoeschst 33342	Life Technology Corporation (Carlsbad, CA)	H1399	IF/IC	1:500

The antibodies are listed along with dilutions used for immunocytochemistry (IC), immunofluorescence (IF), Western blot (WB) analysis. NA, not applicable.

Rockville, MD). PGs were then extracted in hexane/ethyl acetate (1:1) and measured by the liquid chromatography/tandem mass spectrometry method using the Agilent 1200 series high-performance liquid chromatography system and tandem quadrupole mass spectrometry (6460 series; Agilent Technologies, Inc., Santa Clara, CA). PGs of interest were chromatographically separated using a Kinetex 3- μ m C₁₈ 2 \times 100-mm analytic column (Phenomenex, Inc., Torrance, CA). The mobile phase consisted of 0.1% formic acid in water and 0.1% formic acid in acetonitrile using a linear methanol gradient consisting of 20%B to 40%B for 4 minutes and then stay at 40%B for 8.5 minutes, followed by changing from 40%B to 90%B in 12 minutes. This was then increased to 98%B organic concentration over the next 5 minutes and kept at this condition for an additional 4 minutes to achieve chromatographic baseline resolution. The flow rate was 0.4 mL/minute, with a column temperature of 35°C. The mass spectrometer was operated in negative electrospray ionization mode, with source and gas temperatures at 350°C for the analysis of eicosanoids. PGs were detected and quantified by multiple reaction mode monitoring of the transitions of PGs and their relevant internal standards (Cayman Chemical Company).³⁵ PG levels were normalized against tissue protein concentrations.

Cell Viability Assay

Mouse EMC (2 \times 10³ per well) and RL95-2 human EMC (1 \times 10⁴ per well) cells were seeded in a 96-well plate. After culture overnight in Dulbecco's modified Eagle's medium and Ham's F-12 nutrient mixture (1:1) with 10% FBS and antibiotics, the cells were incubated in serum-free medium containing either 0.2% dimethyl sulfoxide (DMSO), rapamycin, or celecoxib. 3-(4,5-dimethylthiazol-2-yl)-5-(3-carboxymethoxyphenyl)-2-(4-sulfophenyl)-2H-tetrazolium (MTS) colorimetric assays per manufacturer's instructions (Promega Corporation, Fitchburg, WI) were monitored at an absorbance of 490 nm as an index of cell viability/proliferation.

Cell Cycle Analysis

Mouse EMC cells (1.0 \times 10⁶ per dish) were plated in 100-mm plates. After culture overnight, the cells were incubated for 2 days in serum-free medium containing either 0.2% DMSO, rapamycin, or celecoxib. Trypsinized cells were fixed with ethanol and treated with propidium iodide and RNaseA. Data were collected and analyzed using a LSRFortessa flow cytometer and FACSDiva version 6.1.3 (BD Immunocytometry Systems, San Jose, CA) or FlowJo version 9.7.5 (Tree Star Inc., Ashland, OR) software.

Apoptosis Assays

Mouse EMC cells (1.0 \times 10⁶ per dish) were plated in 100-mm plates. After culture overnight, the cells were incubated for 3

days in serum-free medium containing either 0.2% DMSO, rapamycin, or celecoxib. Apoptotic cells were identified using a TACS Annexin V-FITC Apoptosis Detection Kit according to the manufacturer's instructions (R&D Systems Inc., Minneapolis, MN). For this assay, the cells were harvested, washed, and incubated with annexin V fluorescein isothiocyanate and propidium iodide. After washing, the cells were analyzed by flow cytometry. Apoptotic cells were also examined by immunofluorescence with anticlaved caspase 3 antibody (Table 1). In brief, 5 \times 10⁴ mouse EMC cells per well were seeded in 8-well chamber slides. After overnight culture, the cells were treated with vehicle (0.2% DMSO), celecoxib, rapamycin, or celecoxib plus rapamycin, for 6 hours in serum-free culture media. Cells were fixed in 4% paraformaldehyde/PBS and immunofluorescence of cleaved caspase 3 was performed (Table 1).

RNA Extraction and RT-PCR

Uterine tissue or EMC cell samples were prepared and analyzed as previously described.^{34,36} In brief, total RNA was extracted with TRIzol according to the manufacturer's protocol (Invitrogen, Carlsbad, CA). After DNase treatment (Ambion Diagnostics Inc., Austin, TX), 1 μ g of total RNA was reverse-transcribed with SuperScript II (Invitrogen). PCR was performed using primers 5'-AGACCATAACC-CACCACAGC-3' and 5'-TACACCAGTCCGTCCTTTC-3' for mouse *Pten*; 5'-ACAGGACCCTGTCACCGAGACC-3' and 5'-GACCTCCGTCATGTGCTGTGAC-3' for mouse *Trp53*; 5'-ACACACTCTATCACTGGCACC-3' and 5'-TTCAGGGAGAAGCGTTTGC-3' for mouse *Ptgs2*; 5'-AGGAGATGGCTGCTGAGTTGG-3' and 5'-AATCTGAC-TTTTCTGAGTTGCC-3' for mouse *Ptgs1*; 5'-GTGGGC-CGCCCTAGGCACCAG-3' and 5'-CTCTTTGATGTCAC-GCAGATTTC-3' for mouse *Actb*; 5'-TGGGAAGCCTT-CTCTAACCTCTCCT-3' and 5'-CTTTGACTGTGGGAG-GATACATCTC-3' for human *PTGS2*; 5'-GAAGAAGT-GGTGCGTAGGGA-3' and 5'-AAGGATTTGGTGTGAG-CGAT-3' for *GUSB*.

Statistical Analysis

The Student's *t*-test was performed to determine the statistical significance of the differences between groups, and the results were reported as statistically significant if the *P* < 0.05 in individual tests.

Results

Endometrial Deletion of *Pten* or Both *Pten* and *Trp53* Up-Regulates Epithelial mTORC1 Signaling

mTORC1 is a downstream target of Akt signaling, which is activated by *Pten* deletion and is associated with EMC.^{9–11} Activation of mTORC1 signaling induces ribosomal protein S6 phosphorylation and is a reliable downstream indicator of heightened mTORC1 signaling.³⁷

We examined the status of pS6 in *Pten*^{d/d} uteri. We found increased levels of pS6 in *Pten*^{d/d} uteri compared with those in littermate floxed uteri at 21 and 30 days of age (Figure 1A and Supplemental Figure S1). However, the levels of pS6 in total uterine extracts were similar between floxed and *Pten*^{d/d} females at 60 and 90 days of age (Figure 1A and Supplemental Figure S1). Interestingly, we observed a higher intensity of pS6 immunolocalization primarily in the uterine epithelia of *Pten*^{d/d} uteri at both 30 and 90 days of age, whereas its expression in floxed uteri was very low and diffused throughout the endometrium (Figure 1C). pS6 is expressed in both the stroma and epithelium in floxed uteri and is regulated by progesterone and estrogen (Supplemental Figure S2). Thus, differences in pS6 levels between floxed and *Pten*^{d/d} uteri were difficult to assess by Western blot analysis after the estrous cycle had started because of the dilution of the protein extracts

with heterogeneous cell types. Heightened levels of pS6 were also observed in *Pten/Trp53*^{d/d} uteri (Figure 1B). mTOR and raptor, which are constituents of mTORC1 complex, were expressed throughout the endometria of both floxed and *Pten*^{d/d} uteri (Figure 1D). These results indicate that mTORC1 function is stimulated only in *Pten*^{d/d} uteri, although mTORC1 machinery exists in both floxed and *Pten*^{d/d} uteri.

PGE₂ and PGD₂ Are Predominantly Produced in *Pten*^{d/d} Uteri

Cox2 is also a downstream target of Akt signaling and is associated with EMC. We previously showed that Cox2 expression is up-regulated in both *Pten*^{d/d} and *Pten/Trp53*^{d/d} uteri.¹⁷ We also showed that Cox2 levels are higher in *Pten*^{d/d} uteri compared with those in *Pten*^{f/f} uteri (Figure 1E).

Cox2-derived PGs are known contributors to cancer growth.^{15,16} Thus, we sought to characterize the PG profile in mouse EMC. We observed that levels of PGE₂ and PGD₂ were much higher in *Pten*^{d/d} uteri than in WT uteri (Figure 1E). High levels of 6-keto-PGF_{1α}, a stable metabolite of PGI₂, were also noted in WT and *Pten*^{d/d} uteri. Levels of PGF_{2α}, 13,14-dihydro-15-keto-PGF_{2α} (13-PGF_{2α}), and 13-PGE₂ were either very low or below the detection limits. Cox2 converts arachidonic acid to PGH₂, which is converted to PGE₂, PGD₂, PGI₂, and PGF_{2α} by their specific PG synthases. The levels of these individual metabolites are dependent on the activities of specific synthases in the defined tissues/cells. The relative lower levels of PGF_{2α} suggest that the expression and activity of PGF_{2α} synthase is limited in the uterus. 13-PGE₂ and 13-PGF_{2α}, which are primary metabolites of PGE₂ and PGF_{2α}, are generated by 15-hydroxy-PG dehydrogenase (15-PGDH). Because both 13-PGE₂ and 13-PGF_{2α} levels are undetectable in both *Pten*^{f/f} and *Pten*^{d/d} uteri, and are lower in *Pten*^{d/d} compared with those in *Pten*^{f/f} uteri, the results suggest that the deletion of *Pten* perhaps decreases the expression or activity of 15-PGDH, a known tumor suppressor in various cancers, including colon, gastric, and lung cancers.^{38–40} Taken together, these results indicate that the *Pten* deletion not only up-regulates Cox2 expression but also down-regulates 15-PGDH, resulting in increased levels of PGE₂ in *Pten*^{d/d} uteri. These results also suggest that Cox2-derived PGE₂ and PGD₂ are major players in EMC. Collectively, both Cox2 and mTORC1 pathways are activated in mouse EMC as observed in human EMC.^{13,41} Although Cox2 and mTORC1 signaling are associated with EMC, it is not known whether they are critical in EMC progression and whether they work in parallel or cooperatively. Thus, we then examined whether treatment with celecoxib and/or rapamycin would attenuate EMC growth in mice.

Cox2 and mTORC1 Inhibitors Compromise EMC in *Pten*^{d/d} and *Pten/Trp53*^{d/d} Females

Pten^{d/d} female mice were treated for 29 days with vehicle, celecoxib, rapamycin, or celecoxib plus rapamycin, starting at 30 days of age, when these mice develop EMC.¹⁷

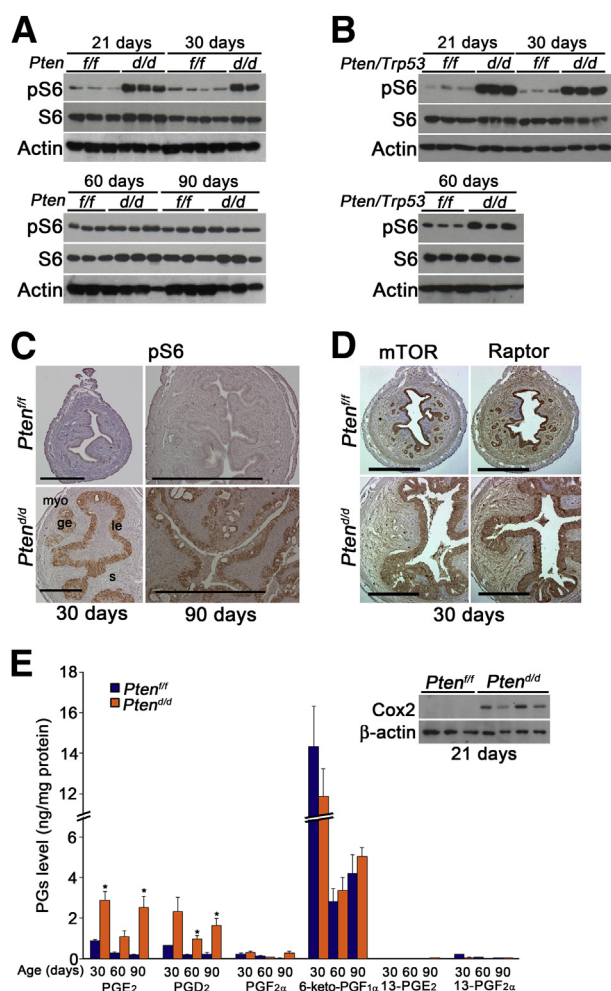


Figure 1 mTORC1 and Cox2 pathways are highly activated in mouse EMC. **A:** Western blot analysis of pS6, an mTORC1 downstream effector, with *Pten*^{f/f} (WT) and *Pten*^{d/d} uteri. **B:** pS6 Western blot analysis with *Pten/Trp53*^{f/f} (WT) and *Pten/Trp53*^{d/d} uteri. **C:** pS6 immunostaining with *Pten*^{f/f} and *Pten*^{d/d} uteri. **D:** IHC analysis of mTORC1 components mTOR and raptor. **E:** Western blot analysis of Cox2 and PG levels with *Pten*^{f/f} and *Pten*^{d/d} uteri. S6 and β-actin served as loading control. **P* < 0.05 versus WT. Scale bars = 400 μm. ge, glandular epithelium; le, luminal epithelium; myo, myometrium; s, stroma.

Although uterine wet weights and sizes were significantly reduced in *Pten^{d/d}* females after treatment with rapamycin or celecoxib alone, they were further attenuated by combined treatment with rapamycin and celecoxib (Figure 2, A and B). The effects of combined treatment (Cel + Rap) appear synergistic because the observed reduction in uterine weight/body weight with celecoxib and rapamycin treatment is less than expected. In addition, mTORC1 and Cox2 signaling pathways can influence each other to affect specific function, suggesting that the effects of the combined treatment are synergistic. We also examined cancer severity by histological analysis (Figure 2C). Although rapamycin treatment markedly reduced the severity of EMC in *Pten^{d/d}* females, treatment with celecoxib had little effect on cancer severity. In contrast, all uteri examined after the combined treatment with celecoxib and rapamycin scored below the highest severity score of 4. These results indicate that celecoxib exacerbates the effects of rapamycin on EMC severity.

We also examined whether these treatments affect EMC in *Pten/Trp53^{d/d}* female mice. Uterine wet weights, sizes, and cancer severity were markedly reduced with rapamycin treatment, whereas celecoxib treatment alone had little effect on these parameters (Figure 3). On the contrary, the combined treatment with celecoxib and rapamycin showed much reduction in uterine wet weights and sizes compared to rapamycin treatment alone. Cancer severity was also attenuated after treatment with both celecoxib and rapamycin, although this finding was not significant when compared with mice receiving only rapamycin treatment. We also examined the effects of celecoxib and rapamycin in *Pten^{f/f}* and *Pten/Trp53^{f/f}*

mice. Although celecoxib treatment alone slightly increased uterine wet weight compared with that with vehicle treatment, this change was much less compared to the effects observed in *Pten^{d/d}* mice (Supplemental Figure S3). In addition, combined treatment with celecoxib and rapamycin did not affect the results of histological examination of the uteri (Figure 2B). All mice treated with rapamycin and/or celecoxib were of body weights more or less similar to those in mice receiving vehicle (Supplemental Table S1). This result suggests that rapamycin and/or celecoxib treatment does not influence body weight. Collectively, these results again indicate that the Cox2 and mTORC1 pathways cooperatively exacerbate EMC. Because the long-term use of high doses of Cox2 inhibitors poses increased cardiovascular risks, and because rapamycin is an immunosuppressant,^{20–29} we used lower doses of celecoxib and rapamycin and used them less frequently. Because of the different metabolic and clearance rates of drugs in mice and humans, the doses of the drugs used in this study cannot directly be compared with those in humans. Notably, we used lower doses of celecoxib and rapamycin (20 and 5 mg/kg body weight, respectively) every alternate day. With these results in hand, we next sought to examine the molecular link between Cox2 and mTORC1 signaling.

Treatment with Celecoxib and/or Rapamycin Reduces Cell Viability in *Pten/Trp53^{d/d}* Mouse EMC Cells and in a Human EMC Cell Line with *PTEN* Mutation

We established a mouse EMC cell line to examine the effects of rapamycin or celecoxib on Cox2 or mTORC1 signaling.

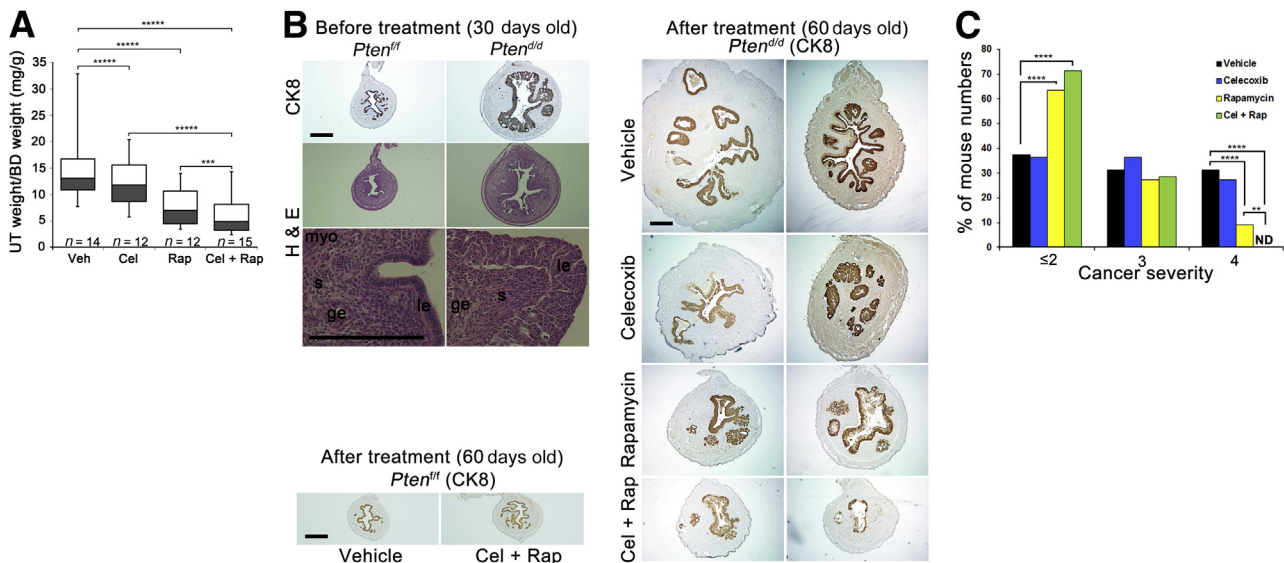


Figure 2 Treatment with celecoxib and/or rapamycin reduces uterine weights and cancer severity in *Pten^{d/d}* mice. *Pten^{d/d}* female mice were treated with vehicle (10% PEG400 and 10% polysorbate 80), 20 mg/kg body (BD) weight Cox2 inhibitor celecoxib (Cel), 5 mg/kg body weight mTORC1 inhibitor rapamycin (Rap), or celecoxib plus rapamycin (Cel + Rap), every alternate day from age 30 to 59 days. Uteri were collected at the age of 60 days. **A:** Uterine (UT) weight from *Pten^{d/d}* mice. The center lines are the medians, the boxes encompass 50% of the data points, and the error bars indicate 100% of the data points. **B:** Immunostaining of an epithelial marker CK8 and hematoxylin and eosin staining. Uterine histological examination from 30-day-old *Pten^{f/f}* and *Pten^{d/d}* mice before treatment and from 60-day-old *Pten^{d/d}* and *Pten^{f/f}* mice with treatment. **C:** Analysis of cancer severity in *Pten^{d/d}* mice. Data are expressed as percentages of mouse numbers scored to each severity. ** $P < 0.01$, *** $P < 0.001$, **** $P \leq 0.0001$, and ***** $P < 0.0001$. Scale bars = 400 μ m. ge, glandular epithelium; le, luminal epithelium; myo, myometrium; ND, not determined; s, stroma.

Epithelial cells were isolated from both *Pten*^{d/d} and *Pten/Trp53*^{d/d} uteri and were seeded in separate dishes to establish mouse EMC cell lines. We found that *Pten*^{d/d} cells attached to plastic dishes, but stopped growing after a few rounds of cell splitting or after freezing with 10% DMSO. In contrast, a *Pten/Trp53*^{d/d} EMC cell line was successfully established, and these cells were able to grow after freezing and thawing. Epithelial cells regrown from frozen stock of *Pten/Trp53*^{d/d} EMC cells were stained with epithelial cell markers E-cadherin and CK8. Epithelial cells from frozen stock of *Pten*^{d/d} EMC did not show E-cadherin or CK8 staining, although sections of *Pten*^{d/d} uteri showed positive staining for these markers in the epithelium (Supplemental Figures S4, A and B). The purity of *Pten/Trp53*^{d/d} cells was >99% (CK8⁺) (Supplemental Figure S5A). The absence of *Pten* and *Trp53* expressions was confirmed by RT-PCR (Supplemental Figure S5B). As expected, the levels of pAkt, Cox2, pS6, and E-cadherin were much higher in these cells (Supplemental Figure S5C). The expression of prostaglandin-endoperoxide synthase 2 (Pgs2), which encodes Cox2, was also confirmed by RT-PCR (Supplemental Figure S5B).

Because *Pten* inactivation was shown to induce cellular senescence through p53 in mouse embryonic fibroblast cells, we examined senescence-associated β -gal staining in uterine epithelial cells.⁴² Interestingly, epithelial cells isolated from *Pten*^{d/d} uteri showed the presence of senescent cells, whereas the cells from *Pten/Trp53*^{d/d} uteri did not show this activity (Supplemental Figure S4C).

Failure to establish a *Pten*^{d/d} epithelial cell line was perhaps due to the fragile nature of these cells that are undergoing senescence. Matrigel support is required to successfully create a primary culture of uterine epithelial cells.⁴³ *Pten/Trp53*^{d/d} cells grew without Matrigel support after three or four passages and could survive >10 passages (data not shown).

Our next objective was to better understand the mechanism that drives inhibition of tumor growth when using rapamycin and celecoxib. We first used MTS assay to evaluate the viability of *Pten/Trp53*^{d/d} mouse EMC cells. Rapamycin or celecoxib reduced the viability of *Pten/Trp53*^{d/d} EMC cells in a dose-dependent manner (Figure 4, A and B). Moreover, combined treatment with rapamycin and celecoxib further reduced cell viability (Figure 4C). We also used a human RL95-2 EMC cell line with *PTEN* and *TP53* mutations.^{44,45} Rapamycin or celecoxib reduced cell viability of RL95-2 EMC cells in a dose-dependent manner (Figure 4, D and E). Celecoxib was more effective in reducing viability in this cell line compared with *Pten/Trp53*^{d/d} mouse EMC cells. However, combined treatment with rapamycin and celecoxib further reduced the cell viability (Figure 4F). We also used a human HEC50B EMC cell line without *PTEN* mutation to examine cell viability by MTS assay.^{44,46} In this cell line, rapamycin or celecoxib did not affect cell viability (Supplemental Figure S6). These results suggest that rapamycin and celecoxib are specifically effective in EMC with *Pten* mutation or *Pten* and *Trp53* mutations.

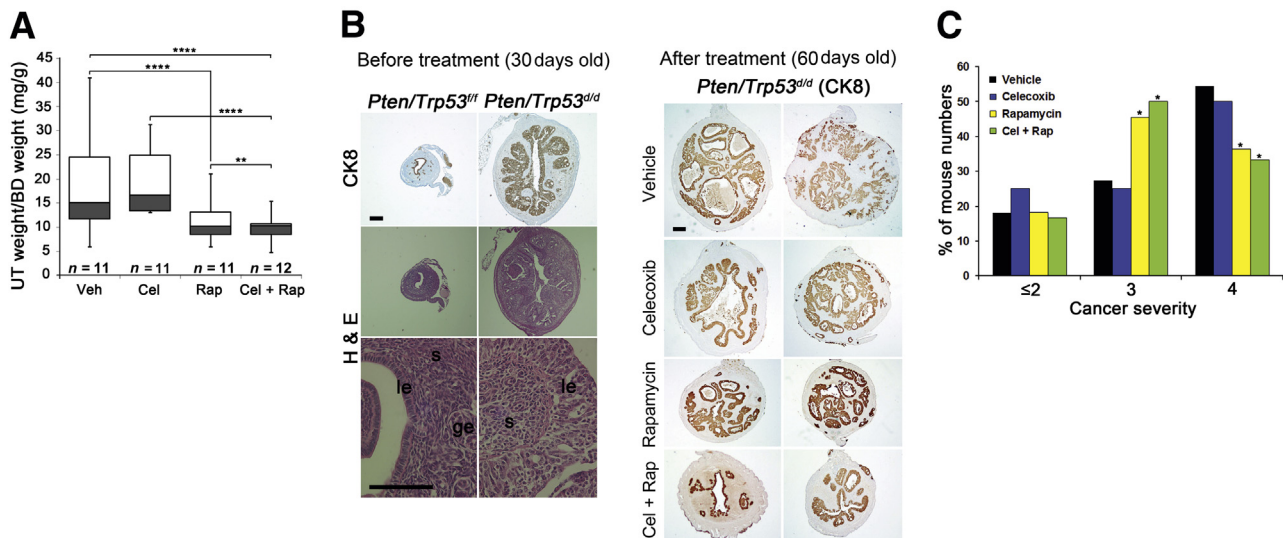


Figure 3 Treatment with rapamycin alone or with rapamycin and celecoxib together reduces uterine weights and cancer severity in *Pten/Trp53*^{d/d} mice. *Pten/Trp53*^{d/d} female mice were treated with vehicle (10% PEG400 and 10% polysorbate 80), 20 mg/kg body weight celecoxib (Cel), 5 mg/kg body (BD) weight rapamycin (Rap), or celecoxib plus rapamycin (Cel + Rap) every alternate day from age 30 to 59 days. Uteri were collected at the age of 60 days. **A:** Analysis of uterine (UT) weight from *Pten/Trp53*^{d/d} mice. The center lines are the medians, the boxes encompass 50% of the data points, and the error bars indicate 100% of the data points. **B:** An epithelial marker CK8 and hematoxylin and eosin staining. Uterine histological examination from 30-day-old *Pten/Trp53*^{f/f} and *Pten/Trp53*^{d/d} mice without any treatment. Uterine histological examination from 60-day-old *Pten/Trp53*^{d/d} mice after treatment. **C:** Analysis of cancer severity from *Pten/Trp53*^{d/d} mice. Data are expressed as percentages of mouse numbers scored to each severity. **P* < 0.05, ***P* < 0.01, and *****P* < 0.0001. Scale bars: 200 μ m (30 days), 400 μ m (60 days). ge, glandular epithelium; le, luminal epithelium; s, stroma.

Rapamycin Attenuates Cell Proliferation, and Celecoxib Accentuates Apoptosis, in EMC

We next used cell cycle and apoptosis assays by culturing *Pten/Trp53^{Δ/Δ}* EMC cells in either the absence or presence of celecoxib, rapamycin, or rapamycin plus celecoxib. Cell cycle analysis by flow cytometry showed that rapamycin arrested cells at the G₀/G₁ phase (Figure 5A), whereas celecoxib had little effect on cell cycle. Interestingly, celecoxib increased the rate of apoptosis, whereas rapamycin did not show such an effect (Figure 5B and Supplemental Figure S7). More importantly, the combined treatment with celecoxib and rapamycin increased the rate of apoptosis compared with celecoxib alone. These results suggest that although both rapamycin and celecoxib decrease cell proliferation, celecoxib alone increases apoptosis; however, rapamycin

increases the rate of apoptosis when combined with celecoxib. These findings were also reflected in the *Pten^{Δ/Δ}* and *Pten/Trp53^{Δ/Δ}* mice treated with celecoxib, rapamycin, or celecoxib plus rapamycin, as examined by proliferation-associated nuclear antigen (Ki-67) and active caspase 3 staining (Figure 5, C and D). The assessment of cell proliferation by Ki-67 staining is an indicator of growth, whereas active caspase 3 staining provides information on the status of apoptotic cells in tissues. Ki-67–positive cells were mainly observed in epithelial cells, which transformed into cancer cells in both *Pten^{Δ/Δ}* and *Pten/Trp53^{Δ/Δ}* uteri (Figure 5C). The populations of Ki-67–positive cells were substantially lower in both *Pten^{Δ/Δ}* and *Pten/Trp53^{Δ/Δ}* mice exposed to rapamycin than in those receiving the vehicle; celecoxib had little effect on cell proliferation. In contrast, active caspase 3–positive (apoptotic) cells were more

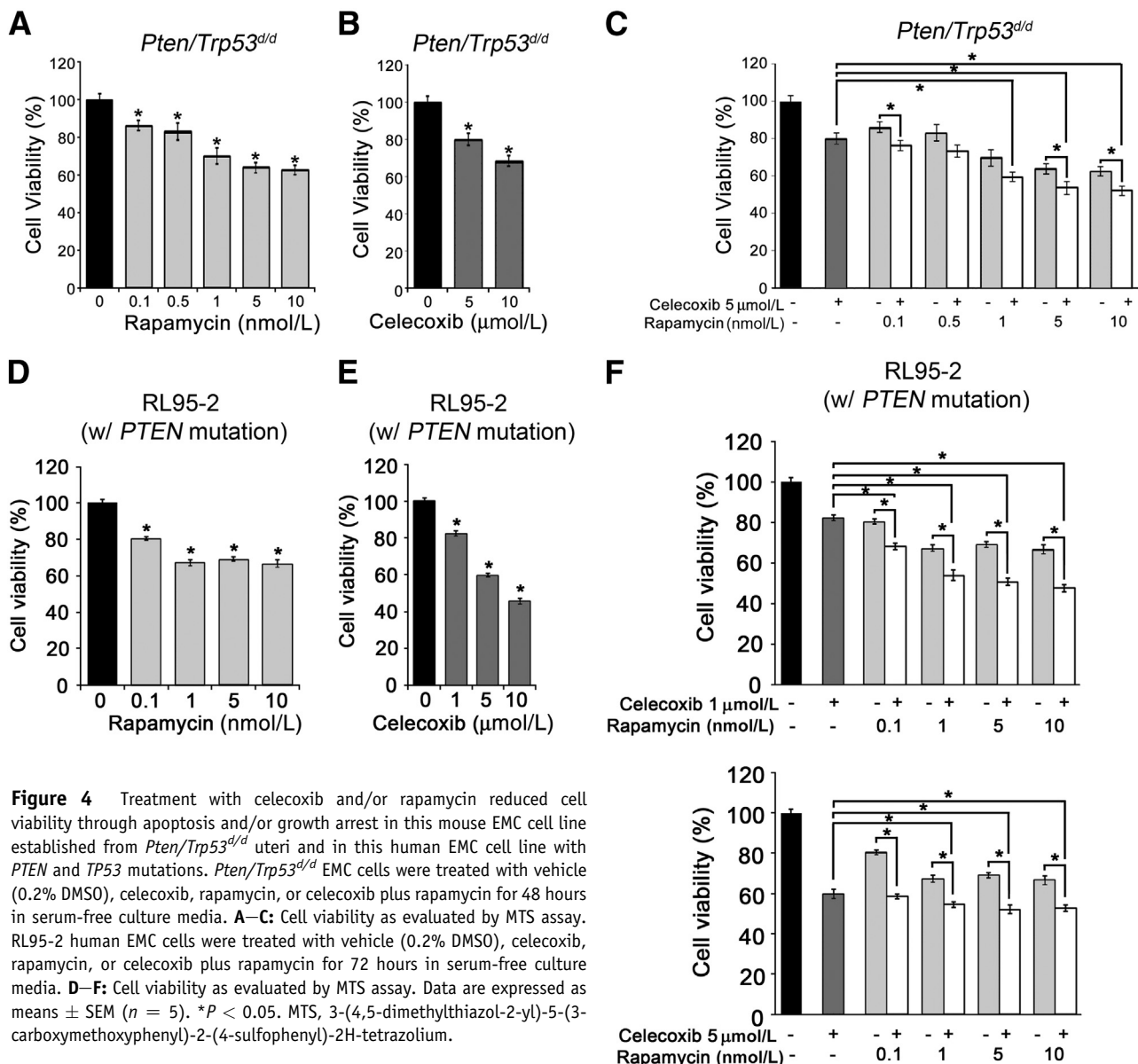


Figure 4 Treatment with celecoxib and/or rapamycin reduced cell viability through apoptosis and/or growth arrest in this mouse EMC cell line established from *Pten/Trp53^{Δ/Δ}* uteri and in this human EMC cell line with *PTEN* and *TP53* mutations. *Pten/Trp53^{Δ/Δ}* EMC cells were treated with vehicle (0.2% DMSO), celecoxib, rapamycin, or celecoxib plus rapamycin for 48 hours in serum-free culture media. **A–C:** Cell viability as evaluated by MTS assay. RL95-2 human EMC cells were treated with vehicle (0.2% DMSO), celecoxib, rapamycin, or celecoxib plus rapamycin for 72 hours in serum-free culture media. **D–F:** Cell viability as evaluated by MTS assay. Data are expressed as means ± SEM ($n = 5$). * $P < 0.05$. MTS, 3-(4,5-dimethylthiazol-2-yl)-5-(3-carboxymethoxyphenyl)-2-(4-sulfophenyl)-2H-tetrazolium.

frequent in EMC sections of celecoxib-treated mice than in those from vehicle-treated mice (Figure 5D). Furthermore, the combined treatment with celecoxib and rapamycin increased the number of active caspase 3—positive cells compared with celecoxib treatment alone.

Cox2 and mTORC1 Activities Are Cross-Regulated and Cooperatively Exacerbate EMC

Our observations suggest that the Cox2 and mTORC1 pathways cooperatively exacerbate EMC, and that celecoxib-

induced apoptosis was further accelerated by the addition of rapamycin. Thus, we speculated that Cox2 and mTORC1 signaling pathways are regulated by each other. We therefore examined the effects of rapamycin or celecoxib on Cox2 or mTORC1 signaling, respectively. In uteri from *Pten*^{d/d} females, treatment with rapamycin every alternate day from 30 to 36 days of age efficiently reduced pS6 levels compared with treatment with vehicle (Figure 6A). Decreased levels of pS6 were also observed in uteri collected from *Pten*^{d/d} mice at 12 hours after a single rapamycin administration (Supplemental Figure S8A). Treatment with 5 nmol/L

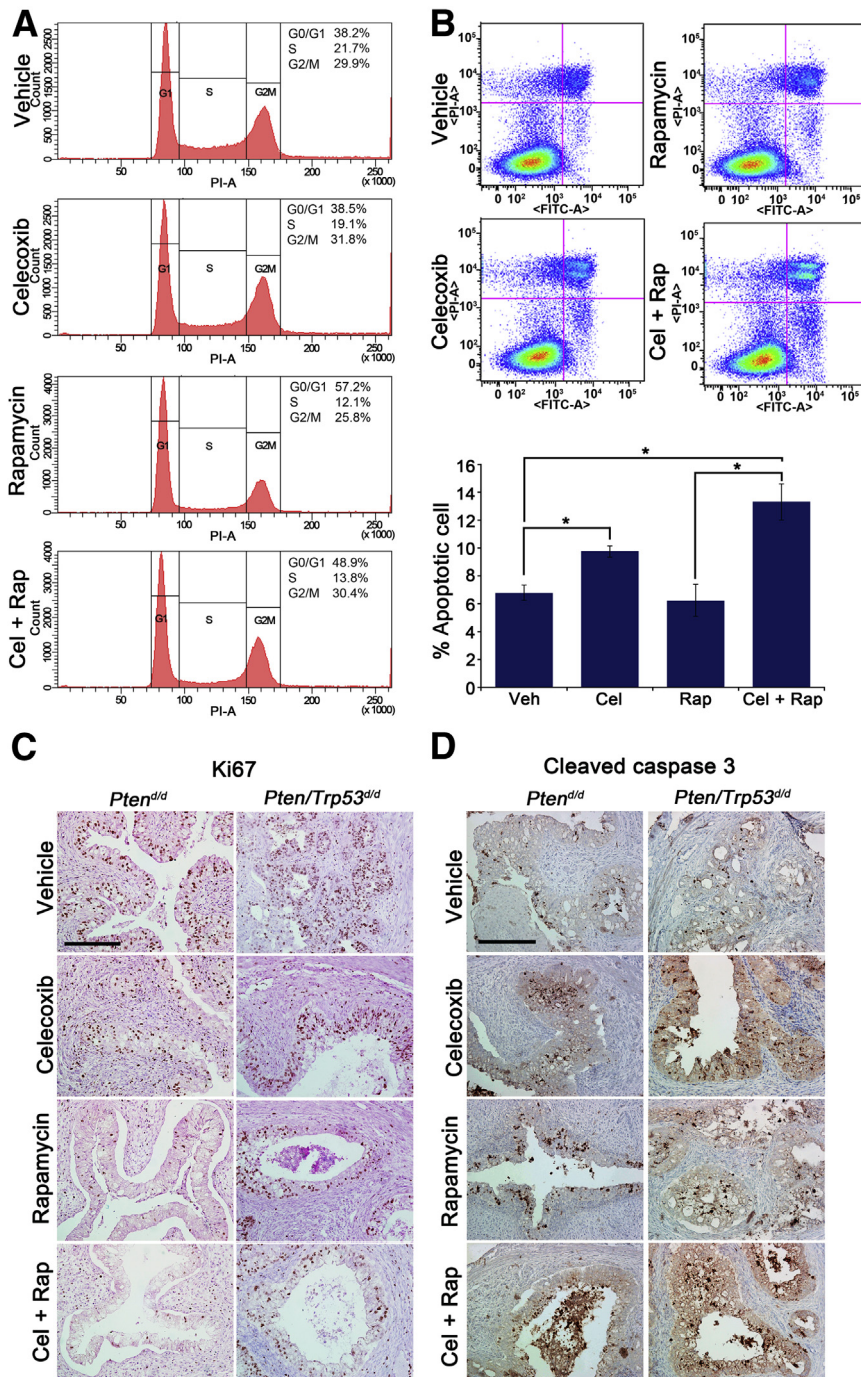


Figure 5 Rapamycin mainly attenuates cell proliferation and celecoxib mainly increases apoptosis in mouse EMC. **A:** Cell cycle was analyzed in *Pten/Trp53*^{d/d} EMC cells stained with propidium iodide (PI) and analyzed by flow cytometry. *Pten/Trp53*^{d/d} EMC cells were treated with vehicle (DMSO), celecoxib, rapamycin, or celecoxib plus rapamycin (Cel + Rap) for 48 hours in serum-free media. **B:** The number of apoptotic cells in *Pten/Trp53*^{d/d} EMC cells was determined by flow cytometry using an Annexin V-FITC kit. *Pten/Trp53*^{d/d} EMC cells were treated with vehicle (Veh) (0.2% DMSO), celecoxib (Cel), rapamycin (Rap), or celecoxib plus rapamycin for 72 hours in serum-free media. **C:** *Pten*^{d/d} and *Pten/Trp53*^{d/d} EMC samples were stained with Ki-67 to evaluate cell proliferation *in vivo*. **D:** *Pten*^{d/d} and *Pten/Trp53*^{d/d} EMC samples were stained with active caspase 3 to evaluate apoptosis *in vivo*. Uterine samples used Ki-67 and caspase 3 immunostaining were derived from mice as described earlier. Data are expressed as means ± SEM ($n = 3$) (**B**). * $P < 0.001$, $n = 3$ (**A**). Scale bars = 800 μm.

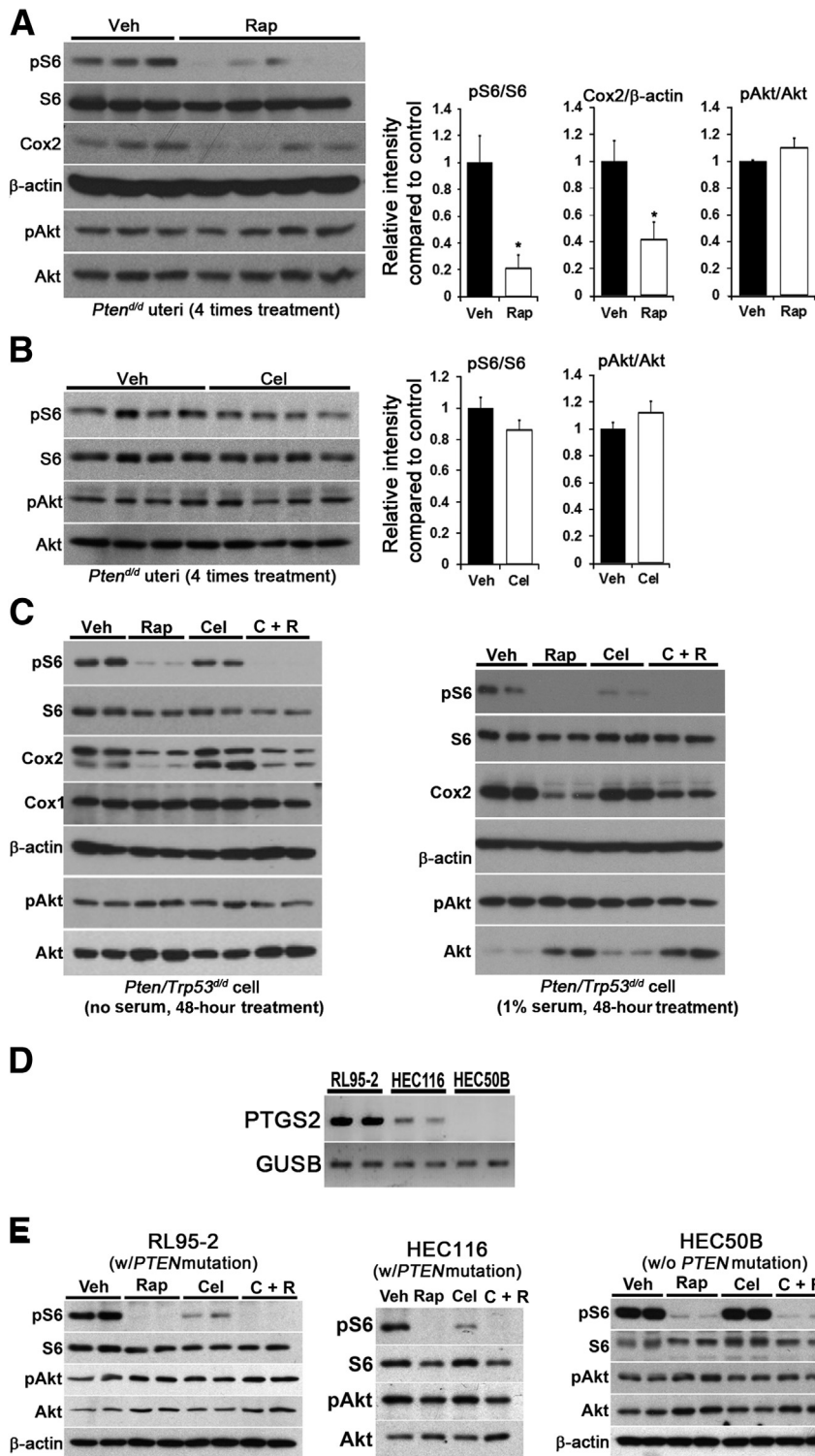


Figure 6 Cox2 and mTORC1 activities are cross-regulated and cooperatively exacerbate EMC. **A** and **B**: Western blot analysis and relative fold changes of band intensities. *Pten^{+/d}* female mice were treated with vehicle (Veh) (10% PEG400 and 10% polysorbate 80) or 5 mg/kg body weight rapamycin (Rap) (**A**) or 20 mg/kg body weight celecoxib (Cel) (**B**), every alternate day from age 30 to 36 days. Quantitatively analyzed band intensities of pS6, Cox2, and pAkt (**A**) and Cox2 and pAkt (**B**) were normalized against total S6, β -actin, and total Akt, respectively (**A**), and β -actin and total Akt, respectively (**B**). Western blot analysis (**C** and **D**) and RT-PCR (**E**) analyses. *Pten/Trp53^{+/d}* EMC cells (1×10^5 per dish) were seeded in a 100-mm dish. **C**: After culture overnight, the cells were treated with vehicle (0.2% DMSO), 5 μ M/L celecoxib, 5 nmol/L rapamycin, or celecoxib plus rapamycin (C + R) for 48 hours in serum-free or 1% FBS-containing media. **D**: PTGS2 expression in RL95-2, HEC116, and HEC50B human EMC cells. GUSB served as an internal control. RL95-2 (6×10^5 per well), HEC116 (3×10^5 per well), or HEC50B (3×10^5 per well) human EMC cells were seeded in a 6-well plate. **E**: After culture overnight, the cells were treated with vehicle (0.2% DMSO), 5 μ M/L celecoxib, 5 nmol/L rapamycin, or celecoxib plus rapamycin for 48 hours in serum-free media. β -actin served as a loading control. * $P < 0.05$.

rapamycin for 48 hours also efficiently reduced pS6 levels in both mouse and human EMC cell lines (Figure 6, C and E). These observations suggest that rapamycin efficiently inhibited mTORC1 activities in our experimental models. However, there is evidence that suppression of mTORC1 can induce feedback activation of Akt in other cancers.^{47,48} Thus,

we examined pAkt levels in *Pten^{+/d}* uteri with and without rapamycin treatment. We found that pAkt levels were not altered by rapamycin treatment, although pS6 levels were reduced (Figure 6A and Supplemental Figure S8A). We also observed that cells in the *Pten/Trp53^{+/d}* mouse and human EMC lines exposed to rapamycin did not alter pAkt levels

(Figure 6, C and E); interestingly, total Akt level increased. The feedback activation of Akt by rapamycin is induced through insulin-like growth factor-1 receptor (IGF-R1). FBS, which includes an IGF-R1 agonist, was used to stimulate this induction in the cell culture system.⁴⁷ However, we did not see Akt activation in *Pten/Trp53^{dd}* mouse EMC cells by rapamycin, even in the presence of 10% FBS (Supplemental Figure S8B). These results suggest that rapamycin fails to induce a feedback activation of Akt in EMC and that rapamycin treatment has great potential to attenuate human EMC resulting from a *PTEN* mutation. We then examined the effects of rapamycin on Cox2 levels. We found that Cox2 levels were reduced after rapamycin treatment in *Pten^{dd}* uteri (Figure 6A). This effect was more clear in *Pten/Trp53^{dd}* EMC cells. We also found that rapamycin reduced Cox2, but not Cox1, expression in mouse EMC cells (Figure 6C; Supplemental Figure S9, A and B). PTGS2 was expressed in human EMC cell lines RL95-2 and HEC116 with *PTEN* mutation (Figure 6D).^{44,49} Decreasing PTGS2 mRNA levels by rapamycin treatment were also observed in RL95-2 cells (Supplemental Figure S9C). These results suggest that the mTORC1 pathway regulates Cox2 expression via transcription and/or translation. However, this regulation occurred only in uteri with malignancy. We previously reported that heightened mTORC1 pathway activity resulting from the deletion of tuberous sclerosis 1 (*Tsc1*), a repressor of mTORC1, did not develop EMC but instead resulted in simple hyperplasia. Interestingly, we found that Cox2 levels were similar or even lower in *Tsc1*-deleted uteri when compared with those in floxed uteri (Supplemental Figure S10). This observation suggests that the mTORC1 signaling regulates Cox2 expression in EMC cells.

We next examined the effects of celecoxib in *Pten^{dd}* uteri and found that celecoxib numerically reduced the pS6 level, although the difference was not significant compared with that in vehicle-treated mouse uteri (Figure 6B). This effect was more clearly evident in mouse *Pten/Trp53^{dd}* and human EMC cell lines RL95-2 and HEC116 with *PTEN* mutations. Celecoxib also reduced pS6 levels in EMC cells (Figure 6, C and E). More importantly, such inhibitory effects of celecoxib were not observed in EMC cells (HEC50B) that did not show PTGS2 expression. Notably, rapamycin plus celecoxib treatment reduced pS6 levels to a greater extent than did treatment with each alone. These results suggest that Cox2 and mTORC1 activities are cross-regulated.

Discussion

This investigation highlights that the Cox2 and mTORC1 pathways regulate each other and have a cooperative role in EMC progression. Thus, the use of a combined treatment with celecoxib and rapamycin may be an effective therapeutic strategy for combating human EMC progression. It is interesting that rapamycin can suppress Cox2 levels and that

celecoxib can suppress pS6 levels (mTORC1 signaling). These observations add new insight into Cox2 and mTORC1 signaling in cancers, although further investigations are required to determine whether and how Cox2 and mTORC1 directly regulate each other. The present study also highlights that rapamycin fails to induce a feedback activation of Akt in EMC, which is unlike the effect of rapamycin in other cancers.

It is known that estrogen exacerbates EMC development, especially during the early stages. Indeed, treatment with high doses of progestin to inhibit unopposed estrogen activity is common during early stages and has been met with reasonable success.¹ However, the drugs available to treat uterine cancers are limited. For example, tamoxifen, an antiestrogen commonly used for breast cancer treatment, has estrogenic effects in the uterus. Long-term treatment with tamoxifen has been shown to increase the risk for EMC.¹ Although spatiotemporal expressions of pS6 and Cox2 are regulated by E_2 and P_4 , we found heightened levels of pS6 and Cox2 in EMC compared with those in normal uterine epithelium. In general, treatment with celecoxib and/or rapamycin reduced cancer severity and uterine weights in mice with EMC, although individual uterine sizes fluctuated within each treatment group. This variation may be a reflection of the additional complexity posed by the differential spatiotemporal expressions of each protein that is regulated by P_4 and estrogen; further studies are necessary to address this issue.

Cox2-derived PGE_2 is known to play important roles in the progression of numerous cancers.¹⁵ In this study, we also observed higher uterine levels of PGE_2 in mice with EMC, which were associated with EMC progression. It will be interesting to see whether PGE_2 can activate the mTORC1 pathway. Another predominant PG product in EMC was PGD_2 . The role of PGD_2 remains unclear; however, some studies have shown that PGD_2 inhibits cancer growth and progression.^{50,51} It is possible that PGD_2 attempts to counter the effects of PGE_2 in EMC, because PGD_2 has opposite effects against PGE_2 in regulating heart rate and body temperature during sleep.⁵² Further investigation is warranted to determine whether PGE_2 and PGD_2 have antagonistic effects in EMC suppression.

Although rapamycin, its analogues, and celecoxib all show beneficial effects for the treatment of EMC and other cancers, there remains the question of how effective these therapies would be in a clinical setting. The long-term usage of high doses of Cox2 inhibitors poses increased risks for cardiovascular complications; meanwhile, long-term use and high doses of rapamycin increase the risk for immunosuppression. Additionally, the potential for feedback activation of Akt, which may in turn lead to increased tumorigenesis, would undermine the effectiveness of rapamycin.^{47,48} In this study, the treatment schedules composed of lower dosages and low frequency of use of a combined rapamycin and celecoxib therapy showed a reduction in EMC progression. These preclinical studies underline the importance of further investigation into the role of celecoxib and rapamycin as a potential treatment strategy for EMC.

Acknowledgments

We thank Serenity Curtis for editing the manuscript, Amanda Bartos and Dustin Sams for expert technical help, and Francesco DeMayo and John B. Lydon (Baylor College of Medicine, Houston, TX) for initially providing the *Pgr-Cre* mice.

Supplemental Data

Supplemental material for this article can be found at <http://dx.doi.org/10.1016/j.ajpath.2014.05.023>.

References

- Di Cristofano A, Ellenson LH: Endometrial carcinoma. *Annu Rev Pathol* 2007, 2:57–85
- Weigelt B, Banerjee S: Molecular targets and targeted therapeutics in endometrial cancer. *Curr Opin Oncol* 2012, 24:554–563
- St-Germain ME, Gagnon V, Mathieu I, Parent S, Asselin E: Akt regulates COX-2 mRNA and protein expression in mutated-PTEN human endometrial cancer cells. *Int J Oncol* 2004, 24:1311–1324
- Sheng H, Shao J, Dubois RN: K-Ras-mediated increase in cyclooxygenase 2 mRNA stability involves activation of the protein kinase B1. *Cancer Res* 2001, 61:2670–2675
- Shao J, Sheng H, Inoue H, Morrow JD, DuBois RN: Regulation of constitutive cyclooxygenase-2 expression in colon carcinoma cells. *J Biol Chem* 2000, 275:33951–33956
- Pommery N, Henichart JP: Involvement of PI3K/Akt pathway in prostate cancer—potential strategies for developing targeted therapies. *Mini Rev Med Chem* 2005, 5:1125–1132
- Guertin DA, Sabatini DM: Defining the role of mTOR in cancer. *Cancer Cell* 2007, 12:9–22
- Liu P, Cheng H, Roberts TM, Zhao JJ: Targeting the phosphoinositide 3-kinase pathway in cancer. *Nat Rev Drug Discov* 2009, 8: 627–644
- Slomovitz BM, Coleman RL: The PI3K/AKT/mTOR pathway as a therapeutic target in endometrial cancer. *Clin Cancer Res* 2012, 18: 5856–5864
- Gadducci A, Tana R, Cosio S, Fanucchi A, Genazzani AR: Molecular target therapies in endometrial cancer: from the basic research to the clinic. *Gynecol Endocrinol* 2008, 24:239–249
- No JH, Jeon YT, Park IA, Kang D, Kim JW, Park NH, Kang SB, Song YS: Expression of mTOR protein and its clinical significance in endometrial cancer. *Med Sci Monit* 2009, 15:BR301–BR305
- Nasir A, Boulware D, Kaiser HE, Lancaster JM, Coppola D, Smith PV, Hakam A, Siegel SE, Bodey B: Cyclooxygenase-2 (COX-2) expression in human endometrial carcinoma and precursor lesions and its possible use in cancer chemoprevention and therapy. *In Vivo* 2007, 21:35–43
- Tong BJ, Tan J, Tajeda L, Das SK, Chapman JA, DuBois RN, Dey SK: Heightened expression of cyclooxygenase-2 and peroxisome proliferator-activated receptor-delta in human endometrial adenocarcinoma. *Neoplasia* 2000, 2:483–490
- Toyoki H, Fujimoto J, Sato E, Sakaguchi H, Tamaya T: Clinical implications of expression of cyclooxygenase-2 related to angiogenesis in uterine endometrial cancers. *Ann Oncol* 2005, 16:51–55
- Wang D, Dubois RN: Eicosanoids and cancer. *Nat Rev Cancer* 2010, 10:181–193
- Turini ME, DuBois RN: Cyclooxygenase-2: a therapeutic target. *Annu Rev Med* 2002, 53:35–57
- Daikoku T, Hirota Y, Tranguch S, Joshi AR, DeMayo FJ, Lydon JB, Ellenson LH, Dey SK: Conditional loss of uterine Pten unfaithfully and rapidly induces endometrial cancer in mice. *Cancer Res* 2008, 68: 5619–5627
- Soyal SM, Mukherjee A, Lee KY, Li J, Li H, DeMayo FJ, Lydon JB: Cre-mediated recombination in cell lineages that express the progesterone receptor. *Genesis* 2005, 41:58–66
- Daikoku T, Yoshie M, Xie H, Sun X, Cha J, Ellenson LH, Dey SK: Conditional deletion of Tsc1 in the female reproductive tract impedes normal oviductal and uterine function by enhancing mTORC1 signaling in mice. *Mol Hum Reprod* 2013, 19:463–472
- Reese J, Zhao X, Ma WG, Brown N, Maziasz TJ, Dey SK: Comparative analysis of pharmacologic and/or genetic disruption of cyclooxygenase-1 and cyclooxygenase-2 function in female reproduction in mice. *Endocrinology* 2001, 142:3198–3206
- Hirota Y, Daikoku T, Tranguch S, Xie H, Bradshaw HB, Dey SK: Uterine-specific p53 deficiency confers premature uterine senescence and promotes preterm birth in mice. *J Clin Invest* 2010, 120:803–815
- Daikoku T, Wang D, Tranguch S, Morrow JD, Orsulic S, DuBois RN, Dey SK: Cyclooxygenase-1 is a potential target for prevention and treatment of ovarian epithelial cancer. *Cancer Res* 2005, 65:3735–3744
- Hirota Y, Cha J, Yoshie M, Daikoku T, Dey SK: Heightened uterine mammalian target of rapamycin complex 1 (mTORC1) signaling provokes preterm birth in mice. *Proc Natl Acad Sci U S A* 2011, 108: 18073–18078
- Tanwar PS, Zhang L, Kaneko-Tarui T, Curley MD, Taketo MM, Rani P, Roberts DJ, Teixeira JM: Mammalian target of rapamycin is a therapeutic target for murine ovarian endometrioid adenocarcinomas with dysregulated Wnt[beta]/catenin and PTEN. *PLoS One* 2011, 6: e20715
- Gulhati P, Zaytseva YY, Valentino JD, Stevens PD, Kim JT, Sasazuki T, Shirasawa S, Lee EY, Weiss HL, Dong J, Gao T, Evers BM: Sorafenib enhances the therapeutic efficacy of rapamycin in colorectal cancers harboring oncogenic KRAS and PIK3CA. *Carcinogenesis* 2012, 33:1782–1790
- Lee N, Woodrum CL, Nabil AM, Rautkys AE, Messina MP, Dabora SL: Rapamycin weekly maintenance dosing and the potential efficacy of combination sorafenib plus rapamycin but not atorvastatin or doxycycline in tuberous sclerosis preclinical models. *BMC Pharmacol* 2009, 9:8
- Wang Z, Zhou J, Fan J, Qiu SJ, Yu Y, Huang XW, Tang ZY: Effect of rapamycin alone and in combination with sorafenib in an orthotopic model of human hepatocellular carcinoma. *Clin Cancer Res* 2008, 14:5124–5130
- Stepkowski SM: Preclinical results of sirolimus treatment in transplant models. *Transplant Proc* 2003, 35(3 Suppl):219S–226S
- Sun ZJ, Zhang L, Hall B, Bian Y, Gutkind JS, Kulkarni AB: Chemopreventive and chemotherapeutic actions of mTOR inhibitor in genetically defined head and neck squamous cell carcinoma mouse model. *Clin Cancer Res* 2012, 18:5304–5313
- Daikoku T, Tranguch S, Friedman DB, Das SK, Smith DF, Dey SK: Proteomic analysis identifies immunophilin FKBP52 as a downstream target of Hoxa10 in the periimplantation mouse uterus. *Mol Endocrinol* 2005, 19:683–697
- Tan Y, Li M, Cox S, Davis MK, Tawfik O, Paria BC, Das SK: HB-EGF directs stromal cell polyploidy and decidualization via cyclin D3 during implantation. *Dev Biol* 2004, 265:181–195
- Kover K, Liang L, Andrews GK, Dey SK: Differential expression and regulation of cytokine genes in the mouse uterus. *Endocrinology* 1995, 136:1666–1673
- Daikoku T, Cha J, Sun X, Tranguch S, Xie H, Fujita T, Hirota Y, Lydon J, DeMayo F, Maxson R, Dey SK: Conditional deletion of Msx homeobox genes in the uterus inhibits blastocyst implantation by altering uterine receptivity. *Dev Cell* 2011, 21:1014–1025
- Daikoku T, Tranguch S, Trofimova IN, Dinulescu DM, Jacks T, Nikitin AY, Connolly DC, Dey SK: Cyclooxygenase-1 is overexpressed in multiple genetically engineered mouse models of epithelial ovarian cancer. *Cancer Res* 2006, 66:2527–2531

35. Yang P, Chan D, Felix E, Madden T, Klein RD, Shureiqi I, Chen X, Dannenberg AJ, Newman RA: Determination of endogenous tissue inflammation profiles by LC/MS/MS: COX- and LOX-derived bioactive lipids. *Prostaglandins Leukot Essent Fatty Acids* 2006, 75:385–395
36. Daikoku T, Tranguch S, Chakrabarty A, Wang D, Khabele D, Orsulic S, Morrow JD, Dubois RN, Dey SK: Extracellular signal-regulated kinase is a target of cyclooxygenase-1-peroxisome proliferator-activated receptor-delta signaling in epithelial ovarian cancer. *Cancer Res* 2007, 67:5285–5292
37. Johnson SC, Rabinovitch PS, Kaeblerlein M: mTOR is a key modulator of ageing and age-related disease. *Nature* 2013, 493:338–345
38. Ding Y, Tong M, Liu S, Moscow JA, Tai HH: NAD⁺-linked 15-hydroxyprostaglandin dehydrogenase (15-PGDH) behaves as a tumor suppressor in lung cancer. *Carcinogenesis* 2005, 26:65–72
39. Liu Z, Wang X, Lu Y, Han S, Zhang F, Zhai H, Lei T, Liang J, Wang J, Wu K, Fan D: Expression of 15-PGDH is downregulated by COX-2 in gastric cancer. *Carcinogenesis* 2008, 29:1219–1227
40. Yan M, Myung SJ, Fink SP, Lawrence E, Lutterbaugh J, Yang P, Zhou X, Liu D, Rerko RM, Willis J, Dawson D, Tai HH, Barnholtz-Sloan JS, Newman RA, Bertagnolli MM, Markowitz SD: 15-Hydroxyprostaglandin dehydrogenase inactivation as a mechanism of resistance to celecoxib chemoprevention of colon tumors. *Proc Natl Acad Sci U S A* 2009, 106:9409–9413
41. Darb-Esfahani S, Faggad A, Noske A, Weichert W, Buckendahl AC, Muller B, Budczies J, Roske A, Dietel M, Denkert C: Phospho-mTOR and phospho-4EBP1 in endometrial adenocarcinoma: association with stage and grade in vivo and link with response to rapamycin treatment in vitro. *J Cancer Res Clin Oncol* 2009, 135: 933–941
42. Chen Z, Trotman LC, Shaffer D, Lin HK, Dotan ZA, Niki M, Koutcher JA, Scher HI, Ludwig T, Gerald W, Cordon-Cardo C, Pandolfi PP: Crucial role of p53-dependent cellular senescence in suppression of Pten-deficient tumorigenesis. *Nature* 2005, 436: 725–730
43. Chung D, Das SK: Mouse primary uterine cell coculture system revisited: ovarian hormones mimic the aspects of in vivo uterine cell proliferation. *Endocrinology* 2011, 152:3246–3258
44. Shoji K, Oda K, Kashiyama T, Ikeda Y, Nakagawa S, Sone K, Miyamoto Y, Hiraie H, Tanikawa M, Miyasaka A, Koso T, Matsumoto Y, Wada-Hiraie O, Kawana K, Kuramoto H, McCormick F, Aburatani H, Yano T, Kozuma S, Taketani Y: Genotype-dependent efficacy of a dual PI3K/mTOR inhibitor, NVP-BEZ235, and an mTOR inhibitor, RAD001, in endometrial carcinomas. *PLoS One* 2012, 7:e37431
45. Berglind H, Pawitan Y, Kato S, Ishioka C, Soussi T: Analysis of p53 mutation status in human cancer cell lines: a paradigm for cell line cross-contamination. *Cancer Biol Ther* 2008, 7:699–708
46. Fujisawa T, Watanabe J, Kamata Y, Hamano M, Hata H, Kuramoto H: VEGF expression and its regulation by p53 gene transfection in endometrial carcinoma cells. *Hum Cell* 2003, 16: 47–54
47. Wan X, Harkavy B, Shen N, Grohar P, Helman LJ: Rapamycin induces feedback activation of Akt signaling through an IGF-1R-dependent mechanism. *Oncogene* 2007, 26:1932–1940
48. Seront E, Pinto A, Bouzin C, Bertrand L, Machiels JP, Feron O: PTEN deficiency is associated with reduced sensitivity to mTOR inhibitor in human bladder cancer through the unhampered feedback loop driving PI3K/Akt activation. *Br J Cancer* 2013, 109: 1586–1592
49. Kamata Y, Watanabe J, Hata H, Hamano M, Kuramoto H: Quantitative study on the correlation between p53 gene mutation and its expression in endometrial carcinoma cell lines. *Eur J Gynaecol Oncol* 2004, 25:55–60
50. Park JM, Kanaoka Y, Eguchi N, Aritake K, Grujic S, Materi AM, Buslon VS, Tippin BL, Kwong AM, Salido E, French SW, Urade Y, Lin HJ: Hematopoietic prostaglandin D synthase suppresses intestinal adenomas in ApcMin/+ mice. *Cancer Res* 2007, 67:881–889
51. Nakamura M, Tsumura H, Satoh T, Matsumoto K, Maruyama H, Majima M, Kitasato H: Tumor apoptosis in prostate cancer by PGD(2) and its metabolite 15d-PGJ(2) in murine model. *Biomed Pharmacother* 2013, 67:66–71
52. Onoe H, Ueno R, Fujita I, Nishino H, Oomura Y, Hayaishi O: Prostaglandin D2, a cerebral sleep-inducing substance in monkeys. *Proc Natl Acad Sci U S A* 1988, 85:4082–4086